

Semiclassical particle-rotor model of one-neutron transfer reactions

R. W. Kincaid,⁽¹⁾ H. Schechter,^(1,2) M. W. Guidry,^(1,4) S. Landowne,^(3,5) R. Donangelo,^(2,5) and G. Leander^{(6),*}

⁽¹⁾*Department of Physics and Astronomy, University of Tennessee, Knoxville, Tennessee 37996*

⁽²⁾*Instituto de Física, Universidade Federal do Rio de Janeiro, Caixa Postal 68528, 21945 Rio de Janeiro, Brazil*

⁽³⁾*Department of Physics, Argonne National Laboratory, 9700 South Cass Avenue, Argonne, Illinois 60439*

⁽⁴⁾*Physics Division, Oak Ridge National Laboratory, Oak Ridge, Tennessee 37831*

⁽⁵⁾*Joint Institute for Heavy Ion Research, Oak Ridge, Tennessee 37831*

⁽⁶⁾*University Isotope Separator at Oak Ridge, Oak Ridge, Tennessee 37831*

(Received 20 July 1992)

We present a model of one-neutron transfer reactions appropriate for cases in which one of the collision partners is deformed. The model considers rotational excitation due to the Coulomb field in the entrance channel, neutron transfer between the two nuclear surfaces at the distance of closest approach, and additional rotational excitation in the final channel. The Coulomb excitation processes are described within the sudden-limit approximation using classical-limit theory, and the transfer is described in terms of spectroscopic amplitudes obtained with the particle-rotor model. We have applied this model of transfer to the $^{58}\text{Ni} + ^{161}\text{Dy}$ and $^{116}\text{Sn} + ^{161}\text{Dy}$ one-neutron pickup reactions, cases for which data are available. The calculations indicate that transfer into both ground and two-quasiparticle excited bands takes place and that the distribution of population in the ground band and two-quasiparticle states is in reasonable agreement with the data.

PACS number(s): 25.70.Hi

I. INTRODUCTION

Transfer reactions induced by light ions have long been useful for investigating properties of low-lying nuclear states. In recent years it has become evident that transfer reactions induced by heavier projectiles can also provide unique probes of nuclei. The charge carried by heavy ions causes strong collective excitation in both the entrance and exit channels, allowing heavy-ion transfer to populate some high-spin states with low single-particle excitation that are not accessible to other reactions. This collective excitation also implies a localization of the transfer reaction in coordinate space, permitting study of details of the nuclear surface. In addition, the transfer takes place between collectively excited states and therefore provides direct information on the single-particle and correlation properties of such states.

Although extending the promise of an important new tool for nuclear studies, heavy-ion-induced transfer reactions have posed some serious experimental problems. Indeed, the traditional methods of light-ion spectroscopy (e.g., use of charged-particle detectors) have proven to be entirely inadequate. In a (d,p) reaction information concerning the energy and angular momentum of the state in which the transferred neutron is left can be extracted from the outgoing proton. But in reactions with more massive projectiles scattering and large energy losses within the target make it very difficult to obtain such information from the collision products. With the development of multidetector γ arrays covering large solid angles, it has, however, become possible to obtain precise

measurements of the spin and energy of the final states; such measurements have been reported in Refs. [1–5], and a review is given in Ref. [6].

Heavy-ion-induced reactions have also presented obstacles to theoretical interpretations. Treatment by standard quantum mechanical coupled-channel methods is complicated because of the extremely large number of relevant states present in both the entrance and exit channels. The long range of the Coulomb interaction as well as the small wavelength associated with relative radial motion provide further motivations for an alternative treatment. Fortunately, the characteristics of heavy-ion reactions that make a quantum mechanical treatment difficult at the same time make the problem amenable to semiclassical methods. A formalism using such techniques to describe one-neutron transfer between two heavy nuclei, one of which is deformed, is developed in Sec. III. Results of applying the model to neutron pickup in the collisions $^{58}\text{Ni} + ^{161}\text{Dy}$ and $^{116}\text{Sn} + ^{161}\text{Dy}$ are presented and compared with the available data in Sec. IV.

II. DESCRIPTION OF THE DATA

Data for one-neutron transfer in these two reactions have been obtained using a particle-particle- γ coincidence method with the Spin Spectrometer at the Holifield Heavy Ion Research Facility of Oak Ridge National Laboratory. Using this almost 4π detector array, the total γ -ray multiplicity and energy associated with a collision event may be measured. The scattering angle and time-of-flight difference for both the recoiling targetlike and projectilelike nuclei were determined in these experiments using position-sensitive parallel-plate avalanche counters placed inside the Spin Spectrometer.

*Deceased.

From this kinematical information it was possible to distinguish the outgoing particles and select a particular reaction process for study.

The data for one-neutron transfer in the $^{58}\text{Ni} + ^{161}\text{Dy}$ collision [1] are summarized by the energy multiplicity plot shown in Fig. 1. The dashed curve represents an approximate yrast line for ^{160}Dy , assuming no excitation of the Ni nucleus. A scale that approximately translates γ -ray multiplicity into the associated value of target angular momentum appears at the bottom of the figure.

Figure 1 indicates that the ^{160}Dy nucleus is left quite cold by this transfer process: most of the population lies within 1–2 MeV of the yrast line. This population is apparently a superposition of two distributions [1]: one is narrow in energy and peaked around $I = 10$; the other is broader in energy, much more intense, and peaked at $I \approx 16$. The bump at lower multiplicity is very near the yrast line and approximately coincides with the maximum for inelastic scattering (of which only the 0.1 contour is shown in the figure) while the second peak lies slightly above the yrast line. In Ref. [1] it was argued that the two regions correspond to different ways, schematically illustrated in Fig. 2, that a neutron may be removed from the ^{161}Dy nucleus. If the unpaired neutron is picked up, the reaction leads to population of the ^{160}Dy ground band (reflected in the lower multiplicity maximum). If any other neutron is removed, the reaction populates an excited two-quasiparticle state (upper multiplicity peak).

Such mechanisms appear to imply that the difference in angular momentum between the two regions populated should be approximately given by the average aligned angular momentum of the two-quasiparticle bands. One

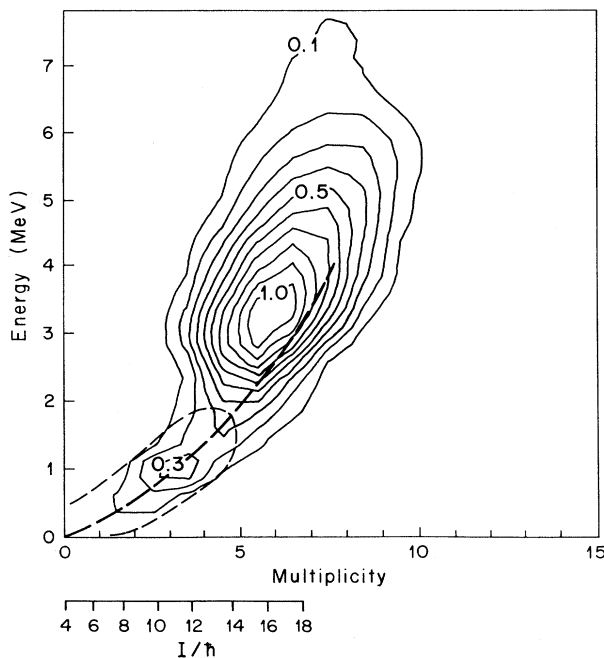


FIG. 1. Experimental total-energy-multiplicity distribution obtained for the one-neutron transfer reaction $^{161}\text{Dy}(^{58}\text{Ni}, ^{59}\text{Ni})^{160}\text{Dy}$ at $E_{\text{Lab}} = 270$ MeV.

1-PARTICLE TRANSFER (ODD MASS)

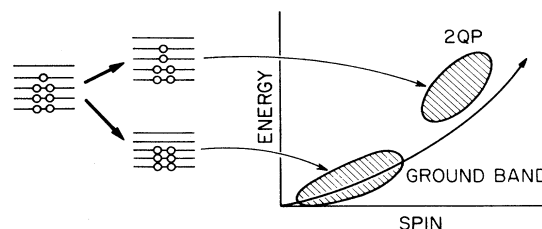


FIG. 2. Schematic representation of two different ways a neutron can be removed from an odd nucleus and the resulting energy and angular momentum of the even- $(A - 1)$ nucleus in each case.

should keep in mind, however, that in all heavy-ion reactions there is considerable collective excitation due to the Coulomb field in both the entrance and exit channel. Since the (E, M) pattern reflects the distribution of *final* states, the peak separation in the data may also be influenced by differing amounts of exit-channel inelastic excitation for nuclei occupying states of the ground and excited two-quasiparticle bands.

A more complete, although still schematic, illustration of the transfer process is given in Fig. 3. There the excitation first proceeds along the ground band of ^{161}Dy as the projectile approaches the target; transfer takes place (into either the ground band or some of the excited two-quasiparticle bands of ^{160}Dy) at the point of closest approach; there is then further inelastic excitation along

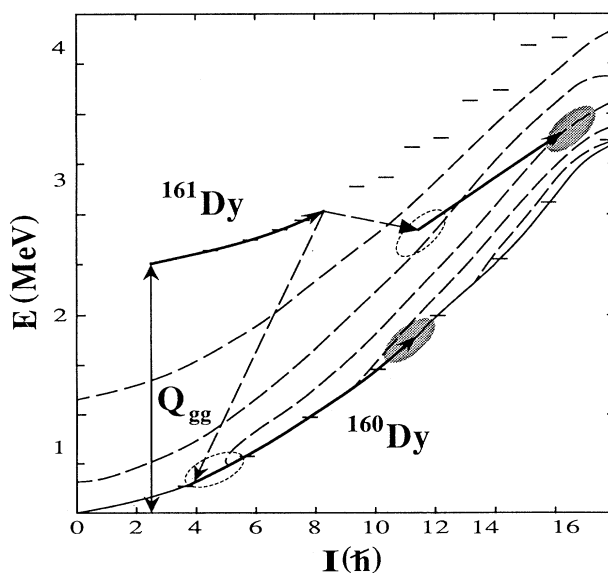


FIG. 3. Three stages of a one-neutron transfer reaction: (i) inelastic excitation of the odd nucleus in the entrance channel; (ii) transfer at the point of closest approach into either the ground band or excited two-quasiparticle bands of the even nucleus; (iii) inelastic excitation in the exit channel. The origin corresponds to the ground state of ^{160}Dy assuming no excitation in the projectilelike nucleus ^{59}Ni . The ground state of ^{161}Dy is displaced from the origin by an energy equal to the ground-state-ground-state Q value.

these bands as the two ions separate. This model has been used previously to give a qualitative understanding of the heavy-ion transfer data summarized in Refs. [1] and [2]. However, to date no quantitative explanation of the general features of high-spin one-neutron transfer has been given. In the following section we develop a quantitative formalism to take these three stages of the reaction process into account.

III. DESCRIPTION OF THE MODEL

In order to be specific, the following discussion is cast in terms of one-neutron pickup by a spherical projectile from a deformed odd- A nucleus. (With only minor modifications, the model can also be applied to one-neutron stripping; we will only point out the necessary changes where they are perhaps not immediately obvious.) We designate a state of the deformed nucleus by its total angular momentum I and its z component (in the laboratory frame) M : $|I_1 M_1\rangle$ is the target nucleus initial state and $|I_2 M_2\rangle$ is the final state of the even- $(A-1)$ targetlike nucleus. The states immediately before and after transfer are denoted as $|I'_1 M'_1\rangle$ and $|I'_2 M'_2\rangle$, respectively. If we assume that the projectilelike nucleus remains in its ground state and that neutron transfer occurs *only* at the classical distance of closest approach, then the amplitude for the entire reaction can be written

$$\begin{aligned} a_{I_1 M_1 \rightarrow I_2 M_2}^{\text{tr}} &= \sum_{\substack{I'_1 M'_1 \\ I'_2 M'_2}} \langle I_2, M_2 | U^+ | I'_2, M'_2 \rangle \langle I'_2, M'_2 | T^0 | I'_1, M'_1 \rangle \\ &\quad \times \langle I'_1, M'_1 | U^- | I_1, M_1 \rangle. \end{aligned} \quad (1)$$

The sum is over complete sets of intermediate states which connect $|I_1 M_1\rangle$ and $|I_2 M_2\rangle$. U^- is the operator providing inelastic excitation in the entrance channel ($-\infty \leq t \leq 0$), U^+ is the analogous quantity for the exit channel ($0 \leq t \leq +\infty$), and T^0 is the operator responsible for one-neutron transfer at the point of closest approach ($t=0$). The superscripts have been chosen to suggest the portions of the trajectory for which the corresponding interactions are relevant.

In the present implementation of our one-neutron transfer model the U^\pm are obtained from the sudden-limit form of the interaction representation's time evolution operator [7]

$$\begin{aligned} \text{entrance: } U^-(\alpha, \beta) &= \exp \left[-\frac{i}{\hbar} \int_{-\infty}^0 V(\alpha, \beta, r(t)) dt \right], \\ \text{exit: } U^+(\alpha, \beta) &= \exp \left[-\frac{i}{\hbar} \int_0^{+\infty} V(\alpha, \beta, r(t)) dt \right]. \end{aligned} \quad (2)$$

Here α and β are respectively the polar and azimuthal orientations of the target's symmetry axis with respect to the laboratory frame, and r is the instantaneous distance of the projectile from the center of the target as illustrated in Fig. 4. The sudden limit is not essential to the method discussed here; U^\pm could be calculated without this restriction, but the computation would then require

the additional complication of time ordering. However, our primary interest at this point is in understanding the *general* features observed in heavy-ion transfer to high-spin states. These should not be very sensitive to the sudden approximation.

For the ion-ion interaction V appearing in Eq. (2) we consider the Coulomb and nuclear contributions:

$$\begin{aligned} V(\chi) &= \frac{Z_p Z_t e^2}{r} + \frac{Z_p Q_2^{(0)} e^2 P_2(\chi)}{2r^3} + \frac{Z_p Q_4^{(0)} e^2 P_4(\chi)}{2r^5} \\ &\quad + \frac{V_0}{1 + \exp\{[r - R_r(\chi)]/a_r\}} \\ &\quad + i \frac{W_0}{1 + \exp\{[r - R_i(\chi)]/a_i\}}, \end{aligned} \quad (3)$$

where $Z_p e$ and $Z_t e$ are the projectile and target charges, and $Q_2^{(0)} e$ and $Q_4^{(0)} e$ are the target quadrupole and hexadecapole moments, respectively. The quantities in the Woods-Saxon parametrization of the complex nuclear potential have their conventional meanings. Figure 4 shows that χ is the angle between the target symmetry axis and the ion-ion line of centers while θ and ϕ are the polar and azimuthal angles of the projectile. For the present calculations we assume the trajectory to lie in the $\phi=0$ plane so the various angles are related through

$$\cos\chi(t) = \cos\alpha \cos\theta(t) + \sin\alpha \cos\beta \sin\theta(t). \quad (4)$$

The one-neutron transfer processes to which we will apply the present model are peripheral. Therefore, although inelastic excitation of the target is governed by

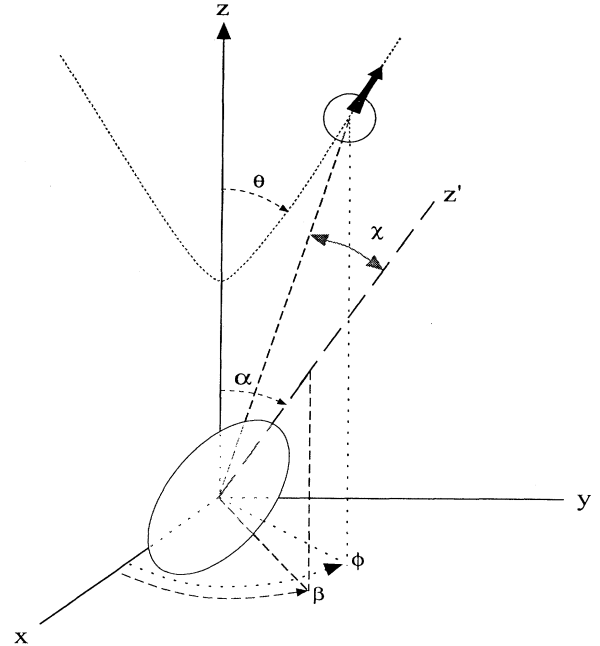


FIG. 4. Coordinates specifying orientation of a deformed target nucleus, position of a spherical projectile, and the angle between the symmetry axis of the target and the ion-ion line of centers.

the interaction potential of Eq. (3), we assume as a first approximation that the projectile path is determined solely by the monopole Coulomb term, $Z_p Z_t e^2/r$. Figure 5 provides a justification for this approximation; there the ratio of the experimental total cross section to the Rutherford value is plotted as a function of scattering angle for a case representative of the experiments we wish to interpret. The conclusions of Refs. [1] and [2] were based on an analysis of the angular region for which this ratio

$$|I, M\rangle = \sqrt{(2I+1)/8\pi^2} \sum_{K\gamma} a_{IK\gamma}^c \left[D_{MK}^I(\alpha, \beta) |K\gamma\rangle + (-1)^{K+I} D_{M, -K}^I(\alpha, \beta) |\bar{K}\gamma\rangle \right], \quad (5)$$

where the $a_{IK\gamma}^c$ result from expanding the intrinsic wave functions in the strong-coupled many-BCS-quasiparticle basis $|K\gamma\rangle$, K being the projection of the total angular momentum I onto the nuclear symmetry axis. The superscript $c = i, f$ is used to make clear whether the coefficient is associated with the wave function in the initial (i) or the final (f) channel, and the quantity γ represents any other quantum numbers needed to specify the state. The collective motion is represented through the rotational wave function $D_{MK}^I(\alpha, \beta)$.

$$\begin{aligned} \xi(I, M, I', M') &= \sum_{K\gamma} a_{IK\gamma}^c a_{I'K\gamma}^c \langle D_{M'K}^{I'} | U | D_{MK}^I \rangle \\ &= \sum_{K\gamma} a_{IK\gamma}^c a_{I'K\gamma}^c \int_0^{2\pi} d\beta \int_0^\pi d\alpha \sin\alpha D_{M'K}^{*I'}(\alpha, \beta) U(\alpha, \beta) D_{MK}^I(\alpha, \beta) \mathcal{F}(\alpha), \end{aligned} \quad (6b)$$

and

$$\mathcal{F}(\alpha) = \begin{cases} 1 & \text{for odd } A \\ e^{-\kappa d(\alpha)} & \text{for even-} A \text{ nuclei} \end{cases} \quad (6c)$$

is a factor representing the effect of the tunneling anisotropy on the angular momentum signature [9]. [The exponential factor in Eq. (6c) arises from consideration of the transfer process—it is the transfer form factor—not the inelastic excitation. But because it is angle dependent it must, if the amplitudes for the three different steps are to be calculated separately, be included in Eq. (6).] It is to be understood that U should be replaced by U^- for

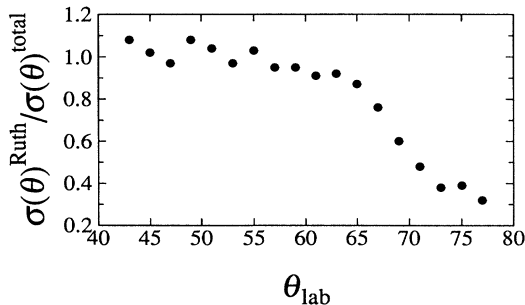


FIG. 5. Ratio of Rutherford and experimental total cross sections for $^{116}\text{Sn} + ^{161}\text{Dy}$ at $E_{\text{Lab}} = 637$ MeV.

was approximately 1. If we also restrict ourselves to this region, we may safely assume that the projectile follows a Rutherford trajectory as we evaluate U^\pm .

The nuclear wave functions that appear in the above amplitudes are calculated for the present work by application of the many-BCS-quasiparticle plus rotor model of Almberger and co-workers [8]. If rotation of the nucleus results in appreciable Coriolis mixing of substrates, the wave function can be written as

Inserting Eq. (5) into the rightmost matrix element of Eq. (1) (for the entrance channel) or the leftmost matrix element (for the exit channel) and taking note of orthogonalities of the $|K\gamma\rangle$ and symmetries of the D functions, we obtain the generic relation

$$\begin{aligned} \langle I', M' | U | I, M \rangle &= \sqrt{(2I+1)/8\pi^2} \sqrt{(2I'+1)/8\pi^2} \\ &\times [1 + (-1)^{2(I+I'-K)+M+M'}] \\ &\times \xi(I, M, I', M'), \end{aligned} \quad (6a)$$

where

the entrance channel or U^+ for the exit channel, and that I, M, I', M' represent the corresponding angular momenta and projections indicated in the rightmost and leftmost matrix elements of Eq. (1). Here $\kappa = \sqrt{2mB_n/\hbar^2}$, with B_n the binding energy of the transferred neutron and m its mass. If B_0 is the binding energy of a particle in the highest occupied orbit (assuming, for convenience, a sharp Fermi surface), then a particle located an energy δ_n below this has a binding energy $B_n = B_0 + \delta_n$. Just after transfer the targetlike nucleus will thus be found in a state with excitation energy δ_n relative to its yrast line, as illustrated in Fig. 6.

The quantity $d(\alpha)$ in Eq. (6c) is the width of the barrier through which a transferred neutron must tunnel. Approximating the target potentials before and after transfer by square wells and assuming transfer to occur only at the point of closest approach (with the transferred neutron restricted to the ion-ion line of centers) gives this barrier width as

$$\begin{aligned} d(\alpha) &= \frac{al^2}{\sqrt{1+l^2-1}} - R_p^0 A_p^{1/3} \\ &\quad - R_t^0 A_t^{1/3} \left[1 + \sqrt{5/4\pi\beta_2} \left(\frac{3}{2} \cos^2\alpha - \frac{1}{2} \right) \right]. \end{aligned} \quad (7)$$

The first term is the minimum distance between centers of the two ions for a Rutherford trajectory with relative orbital angular momentum l ; a is one half the minimum

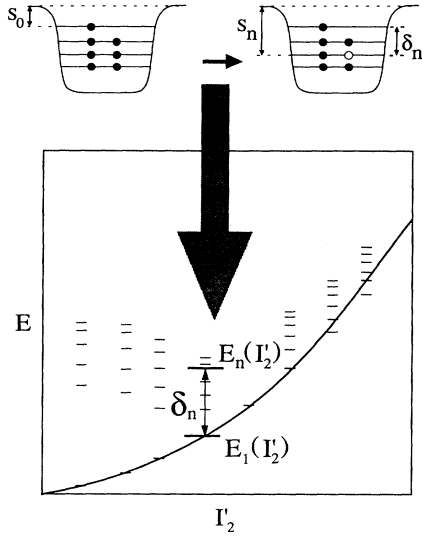


FIG. 6. The energy δ_n appearing in the radial form factor $\exp[-\kappa d(\alpha)]$, where $\kappa = \sqrt{(2m/\hbar^2)(B_0 + \delta_n)}$, in terms of binding energy of a neutron before transfer (top of figure); δ_n is reflected as energy with respect to yrast of the state populated just after transfer (bottom).

distance between ion centers for a head-on collision at center-of-mass energy $E_{c.m.}$, $a = Z_p Z_t e^2 / 2E_{c.m.}$. The second term is the projectile radius, and the third is the radius of the deformed target nucleus at the point on its surface intersected by the ion-ion line of centers (when the target symmetry axis is tilted to an angle α with

$$\langle I_2' || a_j || I_1' \rangle = \sum_{K_1} a_{I_1' K_1}^i \left[\sqrt{2} a_{I_2' 0}^f u_{K_1} \langle I_1' K_1 j - K_1 | I_2' 0 \rangle + (-1)^{I_1' + j + I_2'} \Xi_{K_1}(I_1', I_2') \right], \quad (9)$$

where

$$\begin{aligned} \Xi_{K_1}(I_1', I_2') = & \sum_{\nu_2} [\delta_{\nu_2, K_1} + (-1)^{j-K_1} \delta_{\nu_2, -K_1}] \sum_{\nu_1} (1 + \delta_{K_2, 0})^{-1/2} a_{I_2'; \nu_1 \nu_2}^f v_{\nu_1} \langle I_1' \nu_2 j \nu_1 | I_2' K_2 \rangle \\ & - \sum_{\nu_1} [\delta_{\nu_1, K_1} + (-1)^{j-K_1} \delta_{\nu_1, -K_1}] \sum_{\nu_2} (1 + \delta_{K_2, 0})^{-1/2} a_{I_2'; \nu_1 \nu_2}^f v_{\nu_2} \langle I_1' \nu_1 j \nu_2 | I_2' K_2 \rangle, \end{aligned} \quad (10)$$

with $K_2 = \nu_1 + \nu_2 \geq 0$. The analogous expression for a stripping reaction is obtained by replacing u_{K_1} with v_{K_1} in Eq. (9), v_{ν_1} and v_{ν_2} by u_{ν_1} and u_{ν_2} , respectively, in Eq. (10), and $i \leftrightarrow f$ in both. A replacement of $v \rightarrow -v$ is required in the above expressions if one wishes to make the phases agree with those of Bohr and Mottelson [10]. The coefficients $a_{I_1' K_1}^i$, $a_{I_2' 0}^f$, . . . of Eqs. (9) and (10) are just the $a_{IK\gamma}^c$ of Eq. (5) for the odd and even deformed nuclei.

Once the amplitudes of Eqs. (6) and (8) are obtained for the three separate steps, they are combined according to Eq. (1) to form the total amplitude for the complete one-neutron transfer reaction. Finally, since angular momentum projections were not determined in the experiments of Refs. [1] and [2], we calculate the unpolarized proba-

bility respect to the laboratory z axis). Because one of the ions is spherical, d does not depend on β .

Consideration of the distorted-wave Born approximation suggests that, aside from the radial form factor, the amplitude for transfer of a single neutron between the specific states $|I_1' M_1'\rangle$ and $|I_2' M_2'\rangle$ can be written as

$$\begin{aligned} \langle I_2', M_2' | T^0 | I_1', M_1' \rangle \\ = \sum_j \langle I_2' M_2' j (M_1' - M_2') | I_1' M_1' \rangle \frac{\langle I_2' || a_j || I_1' \rangle}{\sqrt{2I_1' + 1}}. \end{aligned} \quad (8)$$

We shall hereafter refer to the reduced matrix element appearing in this equation as the one-neutron transfer *spectroscopic amplitude*; it provides a quantitative measure of how closely the state of the even nucleus just after transfer resembles the state that would be formed by removing one neutron in a single-particle orbit of angular momentum j from the state occupied by the odd nucleus just before transfer. In addition to using the particle-rotor model wave functions to determine the inelastic excitation via Eqs. (6), they are also required to calculate the $\langle I_2' || a_j || I_1' \rangle$.

The Almberger model assumes that j is a good quantum number in determining the spectroscopic amplitude. This restriction therefore limits the applicability of our own model to those instances in which pickup or stripping proceeds predominantly through transfer of neutrons with one particular value of single-particle angular momentum; we may thus omit the sum over j in Eq. (8).

The spectroscopic amplitude for one-neutron pickup from an odd- A nucleus is given by the Almberger model as

bility

$$P_{I_1' \rightarrow I_2'}^{\text{tr}} = \frac{1}{2I_1' + 1} \sum_{M_1' M_2'} |a_{I_1' M_1' \rightarrow I_2' M_2'}^{\text{tr}}|^2. \quad (11)$$

This is the quantity that we will compare to the data. (Because no effort has been made to include properly normalized wave functions of relative radial motion, P^{tr} is not a true probability in the sense of being limited to the range 0–1. Nevertheless, ratios of this quantity for different values of I_2' in a given reaction are still meaningful, and these are all that are required for our present interests of determining the *relative* likelihood of populating various final states.)

IV. RESULTS AND DISCUSSION

We now investigate applications of the model discussed in Sec. III, first for the reaction $^{161}\text{Dy} (^{58}\text{Ni}, ^{59}\text{Ni})^{160}\text{Dy}$ at $E_{\text{Lab}} = 270$ MeV. Figure 7 illustrates the model's predictions for population of states in the ground band and lowest-lying two-quasiparticle band of ^{160}Dy . Significantly, the calculation indicates population of distinctly different angular momentum regions for these two bands. There is a well-defined peak for the ground band (squares) centered on $I_2 \approx 6$ (from this point onward we drop the subscripts from the notation of Sec. III), while the probability for populating states of the superband exhibits a maximum clearly centered about higher angular momentum ($I \approx 12\hbar$), with a tail extending to very low I . Recall that the experimental (E, M) distribution of Fig. 1 exhibits two distinct maxima, one on the yrast line at low spin and one slightly above the yrast line at higher angular momentum. While the calculated populations are centered at somewhat lower I than the locations of the maxima in the data, the peak separations in experiment and model results roughly agree.

The maximum calculated probability for the superband is only about one-half that of the ground band, while the peak at higher multiplicity in the data is about three times larger than the peak at lower multiplicity. Thus there is a factor of $\approx 6-7$ difference between experimental and calculated peak ratios. One should keep in mind, however, that while there is only one ground band (the primary contributor to the population in the lower angular momentum peak), there are *many* excited two-quasiparticle bands in the energy and angular momentum region that should be populated just after transfer. (A cranked shell-model calculation [1] indicates that there exist at least 6-7 such bands lying within ≈ 1.5 MeV of the yrast line in this angular momentum region.) A more ambitious calculation that includes additional bands could at least qualitatively explain the factor of 6 difference between the calculated superband intensity and the corresponding experimental bump height.

One should, however, exercise caution before claiming

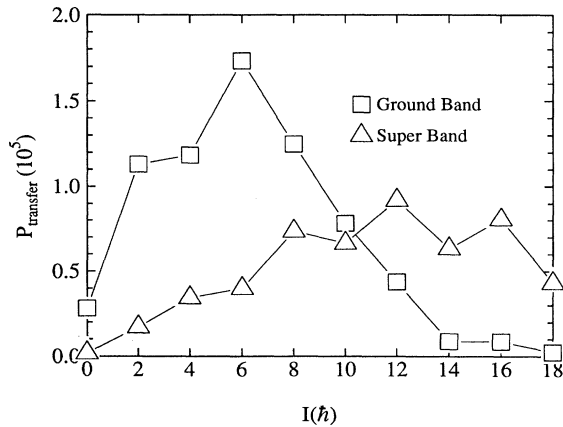


FIG. 7. Calculated probabilities for transfer to the ground band and superband of ^{160}Dy by one-neutron pickup in the reaction $^{58}\text{Ni} + ^{161}\text{Dy}$ at $E_{\text{Lab}} = 270$ MeV.

that such a comparison between peak sizes clearly indicates that 6-7 excited two-quasiparticle bands contribute to the upper (E, M) distribution bump, i.e., that we are actually determining the number of bands involved in this part of the transfer. For one thing, not all of the ^{160}Dy two-quasiparticle bands in this region have the same structure as the superband $[(i_{13/2})^2]$. In addition, the contribution from each of the excited two-quasiparticle bands to the population of the upper peak will be weighted by the exponentially decaying radial form factor, Eq. (6c), that depends on the energy above yrast of the state populated just after transfer. However, the results shown here indicate that a more detailed calculation (using a particle-rotor model or cranked shell model) that takes these factors into account could be used to extract level density information on the intermediate-spin, near yrast region. This is a potentially important result, because it is difficult to obtain such information by other means.

The results of Fig. 7 included no Coriolis attenuation for either of the $^{160,161}\text{Dy}$ nuclei. The lack of attenuation for ^{160}Dy is consistent with the PRM fit to the similar nucleus ^{164}Er by Almerger and co-workers [8]. A one-neutron transfer calculation for $\text{Ni} + \text{Dy}$ has also been made with an imposed attenuation for ^{161}Dy (an *ad hoc* exponent $\rho = 5$ was added to the pairing factor appearing in the Coriolis matrix element according to the prescrip-

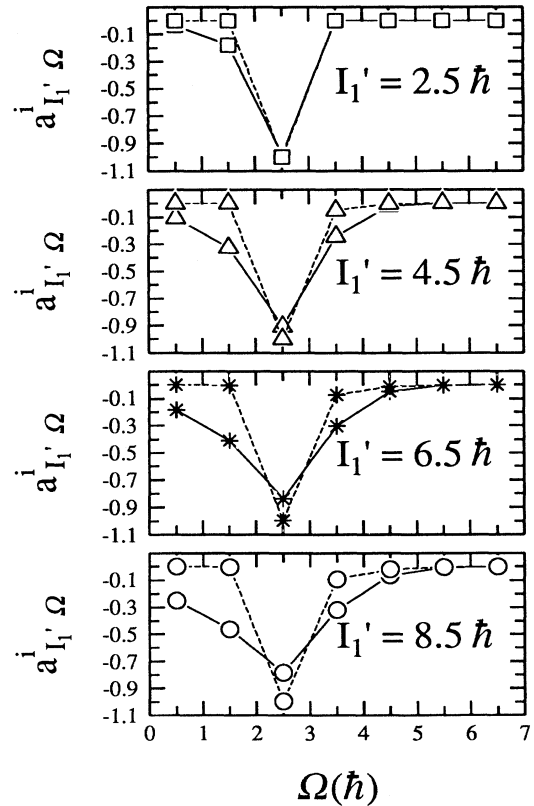


FIG. 8. Particle-rotor model one-quasiparticle wave functions obtained with no Coriolis attenuation (solid lines) and with an exponent $\rho = 5$ added according to the prescription of Ref. [11] (dashed lines).

tion of Ref. [11]). Although the calculated one quasiparticle wave functions show a marked difference in the $\rho=5$ and 0 (no attenuation) cases, as shown in Fig. 8, there is no comparable difference in the results of the corresponding transfer calculations (Fig. 9). We surmise that differences in the individual $1qp$ wave functions are washed out by summation of Eq. (1) over the large number of intermediate states.

We have also applied our model to $^{161}\text{Dy}(^{116}\text{Sn},^{117}\text{Sn})^{160}\text{Dy}$ at a laboratory energy of 637 MeV. The experimental (E, M) distribution for this reaction [2] is shown in Fig. 10, and the results of the calculation are shown in Fig. 11. It is evident that, just as the data for Ni + Dy and Sn + Dy are similar, the calculation for a Sn projectile possesses the same general features as the calculation for a Ni projectile: there is a peak in the ground band population at low angular momentum and one in the superband at higher angular momentum. The higher angular momentum peak in the data (calculation) is larger (smaller) in size than the one at lower angular momentum, which again reflects the fact that a number of excited two-quasiparticle bands are involved in the transfer at large I .

The dip at $I=14$ in the calculated distribution for the superband may be associated with our treatment of the crossing of the ground band by the superband: we have assumed a sharp crossing between $I=14$ and 16 and simply switched the particle-rotor model wave functions and spectroscopic amplitudes for the two lowest-lying states at each angular momentum after $I=14$ before input into Eqs. (6) and (8). The fact that the calculation tends to predict a larger population at the highest spins than is seen in the data is primarily a consequence of our use of the sudden limit for the inelastic excitation. While adequate in the Ni + Dy reaction, this limit is a less good approximation for the Sn + Dy system.

In previous work [12], cross sections have been obtained for transfer to discrete states in the ground band of ^{160}Dy with these same Ni and Sn projectiles. These data are compared with our calculations in Fig. 12 (since the $2^+ \rightarrow 0^+$ transition proceeds largely by internal conver-

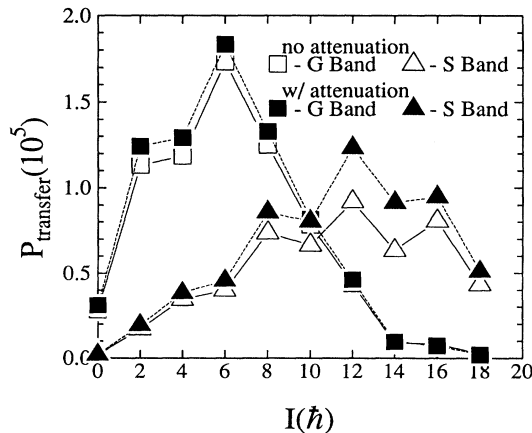


FIG. 9. Calculated one-neutron pickup probabilities with no Coriolis attenuation for the odd- A nucleus (open symbols) and with the attenuation factor of Fig. 8 (filled symbols).

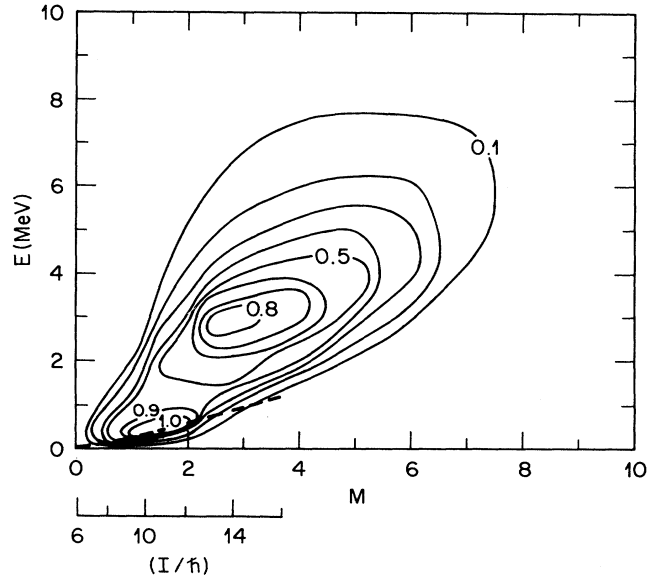


FIG. 10. Experimental total-energy-multiplicity distribution obtained for the reaction $^{161}\text{Dy}(^{116}\text{Sn},^{117}\text{Sn})^{160}\text{Dy}$ at a laboratory energy of 637 MeV.

sion, only $I \geq 4$ is pictured). The experimental differential cross section for a reaction with final scattering angle θ was obtained as the product of the Rutherford cross section at this angle and the experimental probability $P_{\text{exp}}(I)$ of the reaction populating a state of angular momentum I . The experimental quantity plotted in Fig. 12 is this product integrated over a range about the grazing angle; the integral is approximately proportional to $P_{\text{exp}}(I)$ so a direct comparison with the calculated probabilities should be meaningful. The calculations (dashed curves of Fig. 12) include no integration; they are just the ground band results of Figs. 7 and 11 renormalized for each projectile so that the sum of the calculated probabilities is the same as the sum of the experimental cross sections for $I=4, \dots, 18$.

The most important feature of Fig. 12 is that the calculation largely mirrors the trend in data points. In partic-

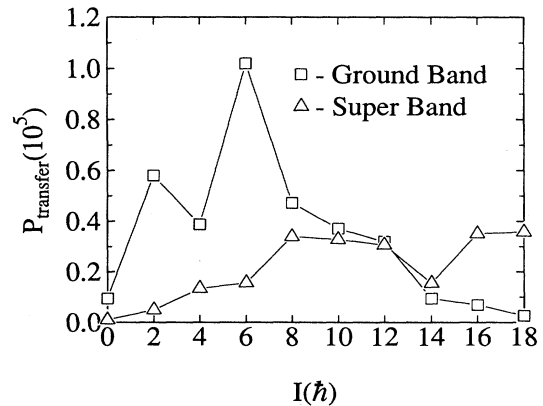


FIG. 11. Calculated probabilities for transfer to the ground band and superband of ^{160}Dy in one-neutron pickup from ^{161}Dy by ^{116}Sn at $E_{\text{Lab}} = 637$ MeV.

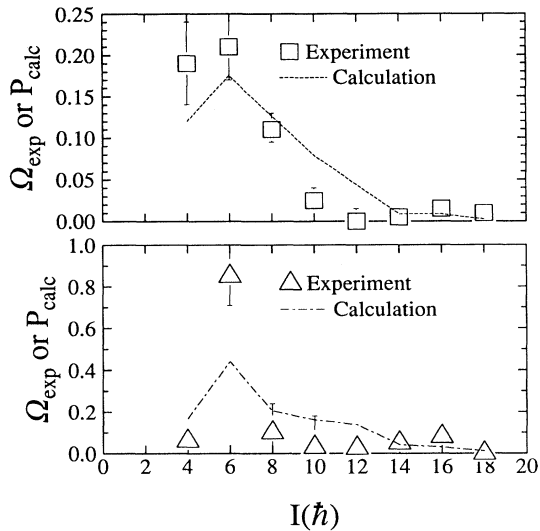


FIG. 12. Comparison of model calculations with experimental cross sections for population of discrete states in the ground band of ^{160}Dy via one-neutron pickup from ^{161}Dy by ^{58}Ni (top) and ^{116}Sn (bottom).

ular, the data for both Ni and Sn projectiles show a ground band maximum at $I=6$, just as in our calculations. Furthermore, the data indicate a much larger difference between the populations of the 4^+ and 6^+ states of ^{160}Dy when the projectile is ^{116}Sn than when it is ^{58}Ni ; a similar, though less pronounced, difference appears in the calculation.

V. CONCLUSION

We have developed a model of one-neutron transfer based on a three-step description that incorporates semiclassical reaction dynamics and a particle-rotor model description of the microscopic nuclear structure. To our knowledge, this represents the most microscopic description yet given for such one-particle heavy-ion transfer reactions populating high-spin states. When applied to the $^{58}\text{Ni} + ^{161}\text{Dy}$ and $^{116}\text{Sn} + ^{161}\text{Dy}$ pickup reactions, this model indicates transfer to a low angular momentum region of the ground band and to a higher angular momentum region of the superband. These results lend support to previous qualitative arguments that the two maxima observed experimentally in the (E, M) distributions reflect transfer to states of ^{160}Dy with different intrinsic structures. The peaks in the calculated distributions occur at

somewhat smaller I than the (estimated) angular momenta of the maxima in the (E, M) distributions, but the peak separations are similar in data and experiment. Furthermore, in both reactions experimental cross sections for transfer to discrete states of the ground band exhibit maxima at $I=6$, the location of the peaks in the corresponding calculations. We argue that differences in peak heights between calculation and (E, M) data may carry information about the approximate number of excited two-quasiparticle bands involved in the transfer at high angular momentum. Thus, a comparison of data with extensive calculations of the kind presented here could yield important information about the near-yrast quasicontinuum region at intermediate spins.

Our approach includes several approximations, and improvements should be considered. In particular, a reliable application of the model to reactions induced by very heavy ions such as ^{116}Sn should not be subject to the limitations of the sudden approximation. While it is not possible to remove these from the present simple model in a rigorous way, given the starting point of the inelastic calculation [i.e., taking Eq. (2) as the form of the inelastic propagator], one could attempt to account for adiabaticity effects—at least approximately—by reducing the target's quadrupole moment according to the prescription of Ref. [13]. More generally, the present method can be reformulated using numerically computed semiclassical propagators that reflect the full dynamics of the inelastic scattering. This is a known technology, and there should be no fundamental difficulties with its implementation. Even before doing this, however, we believe the model provides a schematic understanding of the mechanisms involved in a one-neutron heavy-ion transfer process when one of the reaction partners is deformed.

ACKNOWLEDGMENTS

This work was supported by the U.S. Department of Energy under Contract No. DE-FG05-87ER40361. H.S. and R.D. also thank the CNPq of Brazil for financial support. We all thank the Holifield Heavy Ion Research Facility and the Joint Institute for Heavy Ion Research for their provision of facilities and personnel support. We are grateful for enlightening discussions with J. O. Rasmussen and M. A. Stoyer. In addition, we wish to thank X. T. Liu, S. Juutinen, C. Y. Wu, and D. Cline and his group at the University of Rochester for their contributions in the collection and analysis of data with which the results of our model are compared.

-
- [1] M. W. Guidry *et al.*, Phys. Lett. **163B**, 79 (1985).
 [2] S. Juutinen *et al.*, Phys. Lett. B **192**, 307 (1987).
 [3] C. Y. Wu *et al.*, Phys. Lett. B **188**, 25 (1987).
 [4] X. T. Liu *et al.*, Phys. Rev. C **43**, R1 (1991).
 [5] W. J. Kernan *et al.*, Nucl. Phys. A **524**, 344 (1991).
 [6] C. Y. Wu, W. von Oertzen, D. Cline, and M. W. Guidry,

- Annu. Rev. Nucl. Part. Sci. **40**, 285 (1990).
 [7] K. Alder and A. Winther, *Electromagnetic Excitation: Theory of Coulomb Excitation with Heavy Ions* (North-Holland, Amsterdam, 1975), p. 23.
 [8] J. Almberger, I. Hamamoto, and G. Leander, Phys. Scr. **22**, 331 (1980).

- [9] L. F. Canto, R. J. Donangelo, M. W. Guidry, A. R. Farhan, J. O. Rasmussen, P. Ring, and M. A. Stoyer, *Phys. Lett. B* **241**, 295 (1990).
- [10] A. Bohr and B. R. Mottelson, *Nuclear Structure* (Benjamin, New York, 1975), Vol. 2, p. 648.
- [11] F. S. Stephens and R. S. Simon, *Nucl. Phys.* **A183**, 257 (1972).
- [12] X. T. Liu, Ph.D. dissertation, University of Tennessee, 1988; X. T. Liu *et al.* (unpublished).
- [13] H. Esbensen, S. Landowne, and C. Price, *Phys. Rev. C* **36**, 2359 (1987).